Available online at www.sciencedirect.com
ScienceDirect
Journal of Power Sources 171 (2007) 483–488
JOURNAL OF POWER SOURCES
www.elsevier.com/locate/jpowsour

Short communication

Effect of pyrophosphates as supporting matrices on proton conductivity for NH_4PO_3 composites at intermediate temperatures

Toshiaki Matsui [a], Naoto Kazusa [a], Yukinari Kato [a], Yasutoshi Iriyama [a], Takeshi Abe [a,*], Kenji Kikuchi [b], Zempachi Ogumi [a]

[a] *Department of Energy and Hydrocarbon Chemistry, Graduate School of Engineering, Kyoto University, Nishikyo-ku, Kyoto 615-8510, Japan*
[b] *Department of Materials Science, The University of Shiga Prefecture, Hikone, Shiga 522-0057, Japan*

Received 27 April 2007; received in revised form 11 June 2007; accepted 11 June 2007
Available online 23 June 2007

Abstract

Composite electrolytes of NH_4PO_3/pyrophosphate (NH_4PO_3/ZrP_2O_7, $NH_4PO_3/Sr_2P_2O_7$, and NH_4PO_3/TiP_2O_7) with various molar ratios were fabricated, and their thermal and electrochemical properties were compared at intermediate temperatures. The XRD pattern of $NH_4PO_3/Sr_2P_2O_7$ composite was consistent with a mixed phase of crystalline NH_4PO_3 and $Sr_2P_2O_7$ regardless of the composition ratio, whereas those of the other composites were identical to pyrophosphates. A significant difference in conductivity was observed depending on the supporting matrices of pyrophosphates although each composite contained almost the same molar concentration of NH_4PO_3. Among the composites, NH_4PO_3/ZrP_2O_7 (molar ratio; 1:1) exhibited the highest proton conductivity, which was more than twice that of NH_4PO_3/TiP_2O_7 (1:1). The conductivity of $NH_4PO_3/Sr_2P_2O_7$ (2:1) composite was 2–3 orders of magnitude lower than that of NH_4PO_3/ZrP_2O_7 (1:1). These results suggest that the surface property of pyrophosphates strongly affects the electrochemical properties of composites. Furthermore, a fuel cell that used NH_4PO_3/ZrP_2O_7 composite as an electrolyte was successfully demonstrated at 300 °C.

Keywords: Proton conductor; Intermediate-temperature fuel cells; Pyrophosphate; Ammonium polyphosphate

1. Introduction

Recently, considerable effort has been devoted to develop novel solid state proton conductors for intermediate-temperature applications (100–300 °C) such as fuel cells, sensors and pumps [1–4]. At low temperatures (below 100 °C), hydrated perfluorosulfonic acid membranes such as Nafion® are widely used as electrolytes. However, these materials require water to maintain high conductivity. Thus, complicated water management is one of the major obstacles for intermediate-temperature operation since the relative humidity decreases with an increase in temperature between 100 and 300 °C. Although many heat-resistant polymers with high water-holding capability also have been investigated extensively, usage of polymers derived mainly from organic substances limits the operating temperature below 150 °C. On the other hand, inorganic materials are more thermally stable and several compounds have been reported with relatively high proton conductivity. Among them, oxoacid salts such as CsH_2PO_4 are a class of promising electrolyte at intermediate temperatures [5–9].

Ammonium polyphosphate (NH_4PO_3, APP) is one of the oxoacid salts, which is used as fertilizers and flame retardants. This material shows proton conductivity accompanied with the partial decomposition of NH_4PO_3 into HPO_3 at *ca.* 250 °C even under a dry atmosphere, whereas the resultant compound does not stay in the solid state at intermediate temperatures. Thus, the heterogeneous system is preferable, and several groups have reported the electrochemical properties of the composite electrolyte of $NH_4PO_3/(NH_4)_2SiP_4O_{13}$ [10,11]. Although the compound of $(NH_4)_2SiP_4O_{13}$ serves as a supporting matrix, composite effects have not been considered carefully. In previous reports [12,13], we revealed that the structural change of supporting matrix of $(NH_4)_2MP_4O_{13}$ into MP_2O_7 (M = Ti and Si) occurred at intermediate tempera-

* Corresponding author. Tel.: +81 75 383 2483; fax: +81 75 383 2488.
E-mail address: abe@elech.kuic.kyoto-u.ac.jp (T. Abe).

0378-7753/$ – see front matter © 2007 Published by Elsevier B.V.
doi:10.1016/j.jpowsour.2007.06.060

tures in fuel cell operating condition, resulting in the peculiar ionic-conduction property. The analysis of phosphate anion distribution suggested that not only decomposed phosphate species but also matrix structure affected the proton conduction. Then the pyrophosphate of TiP_2O_7 was used as a new matrix, and the resultant composite of NH_4PO_3/TiP_2O_7 exhibited high conductivity of *ca.* 24 mS cm^{-1} at 250 °C in dry Ar [14]. In this case, almost reversible non-Arrhenius-type temperature dependence was observed. This unique behavior suggested that the interfacial interaction between NH_4PO_3 and TiP_2O_7 should play an important role in the mechanism of proton conduction. Similar interfacial interaction was also reported recently in $CsH_5(PO_4)_2/SiP_2O_7$ composite electrolyte [15,16]. Thus, to elucidate the composite effects of pyrophosphates on proton conductivity will be a useful guide to develop a novel proton conductor at intermediate temperatures. In this study, we aimed to investigate the effects of metal species in pyrophosphate on thermal and electrochemical properties for NH_4PO_3 composites, and pyrophosphates of ZrP_2O_7 and $Sr_2P_2O_7$ were selected. Composite electrolytes of NH_4PO_3/pyrophosphate (NH_4PO_3/ZrP_2O_7, $NH_4PO_3/Sr_2P_2O_7$) with various molar ratios were fabricated, and obtained properties were compared among them and with those for NH_4PO_3/TiP_2O_7 [14]. Furthermore, as a preliminary study, fuel cells were operated at 300 °C with supplying dry gases since there were few reports on such research.

2. Experimental

2.1. Preparation of NH_4PO_3/pyrophosphate composite electrolyte

Ammonium polyphosphate (NH_4PO_3) was synthesized from H_3PO_4 (Nacalai Tesque, Inc., guaranteed reagent), P_2O_5 (Wako Pure Chemical Industries, guaranteed reagent) and $(NH_2)_2CO$ (ICN Biomedicals, Inc., ultrapure) [17]. The supporting matrix of zirconium pyrophosphate, ZrP_2O_7, was prepared by the dehydration of zirconium hydrogenphosphate ($Zr(HPO_4)_2$, Aldrich) at 1100 °C for 24 h in air. Strontium pyrophosphate, $Sr_2P_2O_7$, was prepared by heating strontium hydrogenphosphate ($SrHPO_4$, Aldrich) at 650 °C for 6 h in dry Ar. The X-ray diffraction patterns of the resulting powders were identical to those of NH_4PO_3 of Form I [18], cubic-ZrP_2O_7 [19], and α-$Sr_2P_2O_7$ [20], respectively, as shown in Fig. 1. The composite electrolytes were prepared from the resulting powders in molar ratios of NH_4PO_3: pyrophosphate according to NH_4PO_3/ZrP_2O_7 (1:1) and $NH_4PO_3/Sr_2P_2O_7$ (1:1, 2:1 and 4:1). The mixtures were planetary ball-milled and pressed into pellets. The resulting pellets were then sintered at 400 °C for 10 h under NH_3 gas flow. The density of heat-treated composites was about 90% relative to the theoretical density. The composition ratio of each composite is summarized in Table 1. We can roughly estimate the molar concentration ratio of NH_4PO_3 in the composite by assuming that all of the samples were almost dense; NH_4PO_3/ZrP_2O_7 (1:1): NH_4PO_3/TiP_2O_7 (1:1): $NH_4PO_3/Sr_2P_2O_7$ (2:1): $NH_4PO_3/Sr_2P_2O_7$ (4:1) = 1.0: 1.1: 1.4: 1.8.

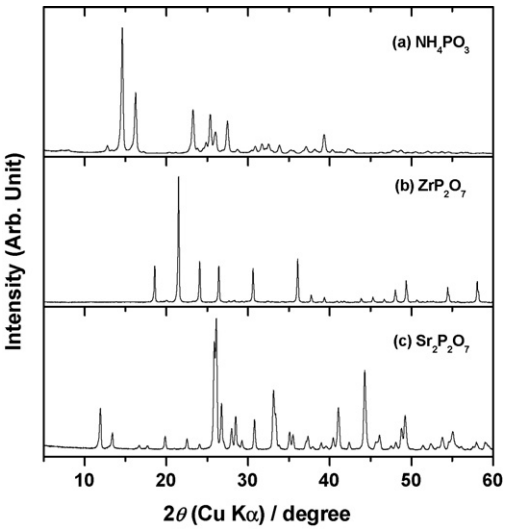

Fig. 1. X-ray diffraction patterns of (a) the obtained NH_4PO_3, (b) ZrP_2O_7, and (c) $Sr_2P_2O_7$.

2.2. Characterization

The structures and the thermal stabilities of the composites were analyzed by X-ray diffraction (Rigaku RINT 2500 X-ray diffractometer) and thermogravimetry (Seiko Instruments Inc., EXTER6000 TG/DTA 6200), respectively. The typical working conditions for XRD were 40 kV and 40 mA, with a scanning rate of 1° min^{-1}. The thermal stability was examined in dry Ar. The zeta potential of matrices was measured with an electrophoretic light-scattering spectrophotometer (Otsuka Electronics, ELS – 800SA). The density of each component was measured by Archimedes' method (Quantachrome, Ultrapycnometer 1000).

2.3. Electrochemical measurements

For electrochemical measurements, Pt/C electrodes (E-TEK, phosphorus acid fuel cell, 1.0 mg cm^{-2}) were used. Proton conductivity was measured by the ac impedance method (Solartron 1260 frequency response analyzer and Solartron 1278 potentiostat) in a temperature range of 150–300 °C under a dry Ar atmosphere. The applied frequency was in the range of 0.1 Hz to 1 MHz with a voltage amplitude of 20 mV. For the evaluation of power generation and transference number, a single cell of Gas (H_2), Pt/C|NH_4PO_3/ZrP_2O_7|Pt/C, Gas (O_2 or H_2/Ar) was fabricated with SUS310S and Gore-tex® Hyper-sheet® gaskets [14]. All samples were measured after being held at 300 °C until a steady state was achieved. Dry hydrogen and oxygen

Table 1
Composition ratio of each composite

Composite	Molar ratio	Volume ratio	Weight ratio
NH_4PO_3/ZrP_2O_7	1:1	0.59	0.37
$NH_4PO_3/Sr_2P_2O_7$	2:1	1.0	0.56
$NH_4PO_3/Sr_2P_2O_7$	4:1	2.1	1.1
NH_4PO_3/TiP_2O_7	1:1	0.69	0.44

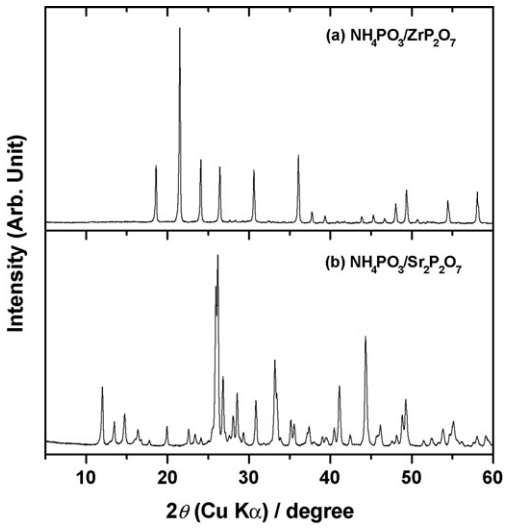

Fig. 2. X-ray diffraction patterns of (a) NH_4PO_3/ZrP_2O_7 (molar ratio; 1:1) and (b) $NH_4PO_3/Sr_2P_2O_7$ (1:1) composite after the heat-treatment at 400 °C for 10 h under an NH_3 atmosphere.

were supplied as a fuel and oxidant under atmospheric pressure, respectively.

3. Results and discussion

3.1. Characterization

The XRD patterns of the NH_4PO_3/pyrophosphate composites (molar ratio; 1:1) that had been heat-treated at 400 °C for 10 h in NH_3 are shown in Fig. 2. In the case of NH_4PO_3/ZrP_2O_7 composite, the pattern was identical to that of cubic-ZrP_2O_7, indicating that NH_4PO_3 was in the amorphous state. Similar results were obtained for NH_4PO_3/TiP_2O_7 composites [14], which resulted from the melting of NH_4PO_3 during the initial heat-treatment at 400 °C. On the other hand, even after heat-treatment, the XRD pattern of $NH_4PO_3/Sr_2P_2O_7$ composite was consistent with a mixed phase of crystalline NH_4PO_3 and $Sr_2P_2O_7$. Regardless of the composition ratio, similar diffraction patterns were obtained. These results should reflect the difference in compatibility between NH_4PO_3 and pyrophosphate at intermediate temperatures. Considering that pure ammonium polyphosphate in the solid state changes into highly viscous material at 400 °C even under an NH_3 atmosphere, the solidification process will be different depending on matrices.

As a typical example, the time-course of weight loss for NH_4PO_3/ZrP_2O_7 (1:1) composite at 300 °C in dry Ar is shown in Fig. 3. The result for each composite is summarized in Table 2. The sample was heated to 300 °C at a rate of 2 °C min^{-1}, and then kept for *ca.* 23 h. In the case of NH_4PO_3/ZrP_2O_7 (1:1) composite, the weight loss reached a steady state with a loss of 7.4%. However, even under a dry condition, this value exceeded the ideal weight loss of 4.7% which was calculated by assuming that NH_4PO_3 decomposed completely into HPO_3. This result indicates that thermal decomposition proceeded with the volatilization of phosphate components. Other

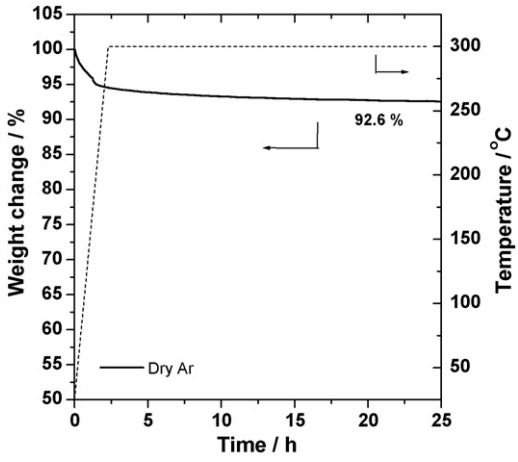

Fig. 3. Time-course of weight loss for NH_4PO_3/ZrP_2O_7 (molar ratio; 1:1) composite at 300 °C in dry Ar (solid line).

composites of $NH_4PO_3/Sr_2P_2O_7$ (2:1) and NH_4PO_3/TiP_2O_7 (1:1) showed similar trend patterns with the weight loss of 9.3% and 5.2%, respectively. To examine the effect of the matrix on thermal stability, the weight change per total weight of NH_4PO_3 was calculated by assuming that each pyrophosphate was stable (Table 2). The composites of NH_4PO_3/ZrP_2O_7 (1:1) and $NH_4PO_3/Sr_2P_2O_7$ (2:1) exhibited almost the same "weight change" although a notable difference was observed in the crystallinity of NH_4PO_3 (Fig. 2). Hence, there is no specific correlation between thermal stability and crystallinity. Moreover, the net "weight change" was not proportional to the estimated molar concentration ratio of NH_4PO_3; the composite of NH_4PO_3/TiP_2O_7 (1:1) exhibited the lowest weight change. Thus, the thermal stability of NH_4PO_3 in the composite appeared to strongly depend on supporting matrices. Throughout this experiment, each composite was kept in the solid state, indicating thermally stable.

3.2. Electrochemical properties

The temperature dependence of proton conductivity for NH_4PO_3/ZrP_2O_7 (1:1) and $NH_4PO_3/Sr_2P_2O_7$ (2:1) composites in dry Ar is shown in Fig. 4. For comparison, the result for NH_4PO_3/TiP_2O_7 (1:1) composite is also shown [14]. Initially, each sample was kept at 300 °C for 24 h until the steady state was achieved. Measurements were then taken under cooling (temperature decreased from 300 to 150 °C) and heating (temperature increased from 150 to 300 °C), as shown as "1st cool" and "2nd heat", respectively. Generally, the conductivity is only proportional to the carrier concentration when the mobility

Table 2
Weight change for each composite at 300 °C

Composite	Molar ratio	Weight loss (%)	Weight change per total weight of NH_4PO_3 (%)
NH_4PO_3/ZrP_2O_7	1:1	7.4	27.6
$NH_4PO_3/Sr_2P_2O_7$	2:1	9.3	26.1
NH_4PO_3/TiP_2O_7	1:1	5.2	17.1

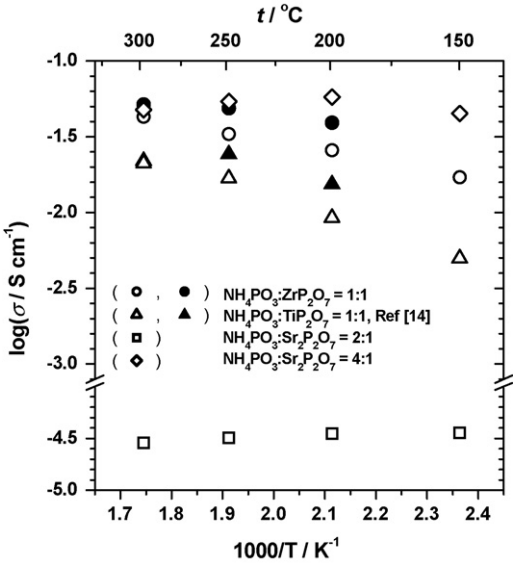

Fig. 4. Temperature dependence of proton conductivity for NH_4PO_3/ZrP_2O_7 (molar ratio; 1:1), $NH_4PO_3/Sr_2P_2O_7$ (2:1 and 4:1), and NH_4PO_3/TiP_2O_7 (1:1) composites [14] in dry Ar: (◯, □, △, ◇) first cooling and (●, ▲) second heating.

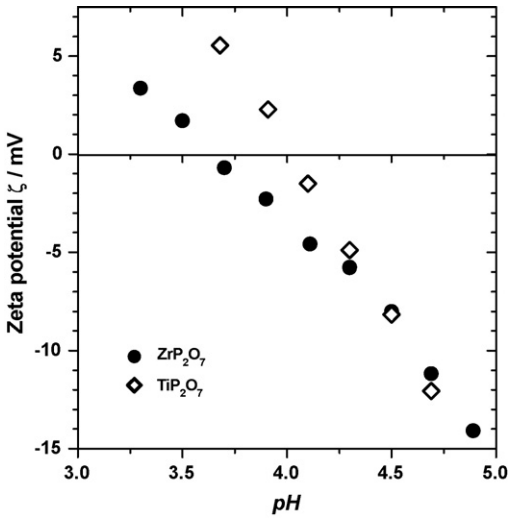

Fig. 5. Zeta potential of ZrP_2O_7 (●) and TiP_2O_7 (◇) as a function of pH.

of charge carrier is constant. This will be true if the conductivity of composite depends on the decomposition ratio of NH_4PO_3 despite matrix species, since each sample contained almost the same concentration of NH_4PO_3: the partially decomposed form of NH_4PO_3 is responsible for high conductivity. However, the conductivity increased in the order of $NH_4PO_3/Sr_2P_2O_7$ (2:1) ≪ NH_4PO_3/TiP_2O_7 (1:1) < NH_4PO_3/ZrP_2O_7 (1:1) at each temperature, which did not agree with the prediction. The conductivity of $NH_4PO_3/Sr_2P_2O_7$ (2:1) was 2–3 orders of magnitude lower than that of NH_4PO_3/ZrP_2O_7 (1:1) with no temperature dependence, regardless of almost the same decomposition ratio of NH_4PO_3. On the other hand, $NH_4PO_3/Sr_2P_2O_7$ composite with a different molar ratio of 4:1 exhibited higher conductivity comparable to that of NH_4PO_3/ZrP_2O_7 (1:1). Thus, an efficient conduction path is not formed in $NH_4PO_3/Sr_2P_2O_7$ (2:1). Furthermore, different proton conduction mechanisms should be proposed between $NH_4PO_3/Sr_2P_2O_7$ (4:1) and NH_4PO_3/ZrP_2O_7 (1:1) considering the notable difference in the temperature dependence of conductivity. Both of these phenomena are quite different from that of pure NH_4PO_3 with an apparent activation energy of *ca.* 0.47 eV, indicating the existence of composite effect. This will be concerned with not only NH_4PO_3 concentration but also the volume ratio of each component such as decomposed phosphate species and matrix as is discussed in the previous paper [13]. The phosphate distribution and their state should be strongly affected by the crystallinity of NH_4PO_3 because of the significant difference in compatibility between NH_4PO_3 and pyrophosphate. Thus, it is revealed that the metal species in pyrophosphate have much effect on proton conduction properties and the conduction phase in the amorphous state is preferable as observed in Fig. 2.

In contrast, the conductivity of NH_4PO_3/ZrP_2O_7 (1:1) was more than twice that of NH_4PO_3/TiP_2O_7 (1:1) although NH_4PO_3 in each composite exhibited good compatibility with pyrophosphates judging from XRD patterns. Moreover, for NH_4PO_3/ZrP_2O_7 (1:1) composite, the temperature dependence of conductivity appeared to be convex upward and to be saturated at *ca.* 300 °C with almost reversible behavior. This non-Arrhenius-type phenomenon is similar to those of NH_4PO_3/TiP_2O_7 composite and $NH_4PO_3/(NH_4)_2SiP_4O_{13}$ composite [11,14]. Especially in the case of NH_4PO_3/TiP_2O_7, this behavior becomes prominent at a low molar ratio of NH_4PO_3. This was attributed to that the interface of amorphous polyphosphate/TiP_2O_7 played an important role. Then, the zeta potential of pyrophosphates was measured to examine the influence of the matrix surface, as shown in Fig. 5. The isopotential points of ZrP_2O_7 and TiP_2O_7 were *ca.* pH 3.6 and 4.0, respectively, indicating that the surface of ZrP_2O_7 was negatively charged. Accordingly, the surface basicity of pyrophosphate strikingly affected the thermal stability of composite, resulting in a difference in the carrier concentration as is discussed in the previous section. In these composites, decomposed phosphate serves as an acid medium. Thus, non-Arrhenius-type behavior in conductivity should also be caused by the acid–base interaction at the interface between the conduction phase and matrix. Since the surface charge is dependent on matrix species, the activation energy in interfacial proton conduction should be different. At this stage, however, the proton conduction mechanism at the interface has not been elucidated sufficiently and is under investigation. The optimized interfacial interaction and structure will provide the fast conduction path.

Hereafter, the composite electrolyte of NH_4PO_3/ZrP_2O_7 (1:1) was used in a fuel cell since it exhibited the highest conductivity of 51 mS cm^{-1} at 300 °C. The Nernstian potential of a hydrogen concentration cell at 300 °C is shown in Fig. 6. The experimental value agreed well with the theoretical one at a high partial pressure of hydrogen. However, the gap between these two values increased with an increase in the concentration gradient, and the apparent transference number was calculated to be 0.83. This value is slightly lower than that of NH_4PO_3/TiP_2O_7

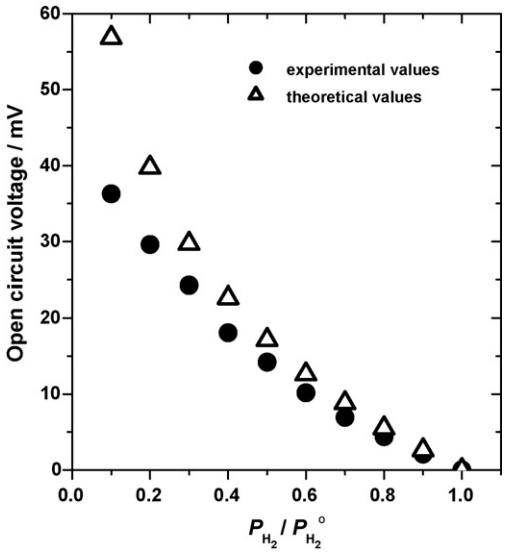

Fig. 6. Nernstian potential of a hydrogen concentration cell using NH_4PO_3/ZrP_2O_7 (molar ratio; 1:1) composite electrolyte at 300 °C: (●) experimental values and (△) theoretical values.

(1:1) at 250 °C [14]. This should be caused by the low density of heat-treated pellets and subsequent NH_3 elimination at 300 °C, resulting in the leakage of gas through the electrolyte under a high concentration gradient. However, this will be improved by optimizing the fabrication method.

The power generation characteristics of a single cell using NH_4PO_3/ZrP_2O_7 composite at 300 °C are shown in Fig. 7. The electrolyte thickness was 2.2 mm. Dry hydrogen and oxygen were supplied as a fuel and oxidant, respectively. The open circuit voltage was 0.72 V, which was somewhat lower than the theoretical value of 1.13 V because of the low relative density of the electrolyte as mentioned above. However, it was possible to generate electricity up to 151 mA cm^{-2}, and the maximum power density was 27 mW cm^{-2}. This performance is comparable to that of NH_4PO_3/TiP_2O_7 composite, and it has been reported that performance limitations are dominantly due to the electrolyte thickness [14]. Thus a dense and thin electrolyte should dramatically improve the performance. This composite electrolyte has the possibility to realize the water-free fuel cell system, which will be the breakthrough technology for use in both stationary and mobile applications. However, there are many points to be elucidated and improved for the development and is under investigation.

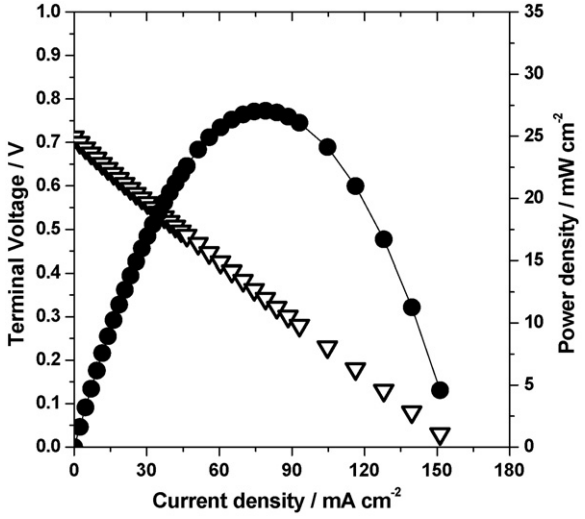

Fig. 7. Cell voltage (open triangles) and power density (filled circles) as a function of current density at 300 °C. [H_2, Pt/C|NH_4PO_3/ZrP_2O_7 (molar ratio; 1:1)|Pt/C, O_2].

4. Conclusions

Composite electrolytes of NH_4PO_3/pyrophosphates were fabricated, and their thermal and electrochemical properties were compared at intermediate temperatures. The metal species in pyrophosphate have much effect on the compatibility with NH_4PO_3, resulting in the different proton conduction mechanism. X-ray diffraction analysis is a convenient method to provide the information on the compatibility, and the amorphous state of NH_4PO_3 appears to be preferable for fast proton conduction. It is also clarified that a difference in the surface basicity of pyrophosphate strongly affects the thermal stability and conductivity due to the acid–base interaction at the interface. Therefore, the optimization of interfacial interaction and structure is useful in the design of novel ionic conductors with high mechanical strength at intermediate temperatures.

Acknowledgements

This work was supported by Research and Development of Polymer Electrolyte Fuel Cell of New Energy and Industrial Technology Development Organization (NEDO), and also by a Grant-in-Aid for the 21st COE program for a United Approach to New Materials Science from the Ministry of Education, Culture, Sports, Science and Technology.

References

[1] B.C.H. Steele, A. Heinzel, Nature 414 (2001) 345.
[2] P. Costamagna, S. Srinivasan, J. Power Sources 102 (2001) 242.
[3] P. Colomban, Proton Conductors: Solids, Membranes and Gels-Materials and Devices, Cambridge University Press, New York, 1992.
[4] T. Norby, Solid State Ionics 125 (1999) 1.
[5] S.M. Halie, D.A. Boysen, C.R.I. Chisholm, R.B. Merle, Nature 410 (2001) 910.
[6] A.I. Baranov, B.V. Merinov, A.V. Tregubchenko, V.P. Khiznichenko, L.A. Shuvalov, N.M. Schagina, Solid State Ionics 36 (1989) 279.
[7] W. Bronowska, J. Chem. Phys. 114 (2001) 611.
[8] J. Otomo, N. Minagawa, C. Wen, K. Eguchi, H. Takahashi, Solid State Ionics 156 (2003) 357.
[9] V.G. Ponomareva, G.V. Lavrova, Solid State Ionics 145 (2001) 197.
[10] T. Kenjo, Y. Ogawa, Solid State Ionics 76 (1995) 29.
[11] M. Cappadonia, O. Niemzig, U. Stimming, Solid State Ionics 125 (1999) 333.
[12] T. Matsui, S. Takeshita, Y. Iriyama, T. Abe, Z. Ogumi, Electrochem. Commun. 6 (2004) 180.
[13] T. Matsui, S. Takeshita, Y. Iriyama, T. Abe, Z. Ogumi, Solid State Ionics 178 (2007) 859.
[14] T. Matsui, S. Takeshita, Y. Iriyama, T. Abe, Z. Ogumi, J. Electrochem. Soc. 152 (2005) A167.

[15] T. Matsui, T. Kukino, R. Kikuchi, K. Eguchi, Electrochem. Solid-State Lett. 8 (2005) A256.
[16] T. Matsui, T. Kukino, R. Kikuchi, K. Eguchi, Electrochim. Acta 51 (2006) 3719.
[17] S. Ueda, K. Oyama, K. Koma, Kogyo Kagaku Zasshi 66 (1963) 589.
[18] C.Y. Shen, N.E. Stahlheber, D.R. Ryroff, J. Am. Chem. Soc. 91 (1969) 62.
[19] JCPDS File Card no. 24-1490.
[20] JCPDS File Card no. 24-1011.